NASA CR-54914
W&S TR-40

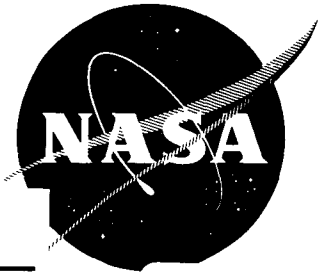

USE OF INFRARED BAND MODELS TO DETERMINE H_2O AND CO_2 CONCENTRATIONS IN SITU AT HIGH TEMPERATURES

GUNTER J. PENZIAS

PREPARED FOR
NATIONAL AERONAUTICS AND SPACE ADMINISTRATION
CONTRACT NAS 3-6282

THE WARNER & SWASEY COMPANY
CONTROL INSTRUMENT DIVISION
32-16 DOWNING STREET
FLUSHING, NEW YORK 11354

NASA CR-54914
W&S TR-40

FINAL REPORT

USE OF INFRARED BAND MODELS TO DETERMINE H_2O AND CO_2 CONCENTRATIONS IN SITU AT HIGH TEMPERATURES

Gunter J. Penzias

Prepared for

NATIONAL AERONAUTICS AND SPACE ADMINISTRATION
Lewis Research Center
Cleveland, Ohio

February 12, 1966

Contract NAS 3-6282

Technical Management
NASA Lewis Research Center
T. Male

THE WARNER & SWASEY COMPANY
CONTROL INSTRUMENT DIVISION
32-16 Downing Street
Flushing, New York 11354

FOREWORD

This report was prepared as part of the task under NASA Contract NAS 3-6282, with NASA Lewis Research Center. Mr. Theodore Male was Technical Manager for NASA.

The author would like to acknowledge the many individuals in this laboratory who assisted in this research effort. Lothar Klein obtained the CO_2 shock tube data. The high resolution measurements were made under the supervision of H. J. Babrov by B. S. Rao. The gas cell measurements and much of the data reduction were done by A. L. Shabott.

ABSTRACT

The statistical band model was used to establish quantitative relationships for use in combustion gas analysis, in situ, for propulsion research applications. The necessary band model parameters, to relate infrared transmittance to CO_2 and H_2O concentrations were determined from 600°K to 2500°K at 4.40-μ for CO_2 and at 2.506-μ and 2.854-μ for H_2O.

Improvements in the technique for determining H_2O concentrations, using integrated absorptance methods, and possible modification of the statistical model relationships, were investigated.

The effects of non-absorbing broadening gases on concentration determinations were also considered.

TABLE OF CONTENTS

LIST OF TABLES

LIST OF ILLUSTRATIONS

I. INTRODUCTION

Techniques to determine concentrations of chemical species in a hot gas, without the need for removing a sample or disturbing the flow, are desirable for many applications, such as the study of rocket nozzle kinetics, supersonic combustion, and chemical reactions in shock tubes. In previous work, we tested infrared combustion gas analysis in situ by determining concentrations of carbon dioxide in a combustion gas from measurements of infrared spectral absorptance (1). A calibration curve obtained by measuring the absorptance of carbon dioxide heated in a gas cell, was used to determine the CO_2 concentrations in the combustion gas (1).

To use a purely empirical approach of setting up calibration curves for infrared analysis in situ would require an impracticably large number of experimental measurements for all possible temperatures, pressures, and mixture ratios. To reduce the amount of data required, use was made of the theory of infrared band models (2). We applied band model theory first to describe the absorptance of CO_2 at constant temperature (3) and then to include the variation of temperature (4). The band model which best correlated the experimental data (3) was the statistical model (2) with random line spacing, constant intensities, and constant widths. A similar band model relationship was obtained for water vapor at one temperature (4). Using the band model approach for determining combustion gas concentrations in situ, CO_2 concentrations were determined in shock-heated gases (5).

In the present work, we measured additional band model data for CO_2 and H_2O, and extended the band model relationship for H_2O to include temperature variations. Improvements to the water vapor band model were also investigated.

The band models and the required parameters are reviewed in Section II. Methods to measure CO_2 and H_2O band model parameters and the results obtained are described in Sections IV and V. The use of integrated absorptance for determination of water vapor concentration is discussed in Section VI. The influence of optically inactive species in the combustion gas is considered in Section VII.

II. STATISTICAL BAND MODEL RELATIONSHIP

Detailed mathematical derivations of the statistical model based upon spectroscopic considerations have been given by Goody (2), Plass (6) and Oppenheim (7). The resulting equations

USE OF INFRARED BAND MODELS TO DETERMINE H_2O AND CO_2 CONCENTRATIONS IN SITU AT HIGH TEMPERATURES

Gunter J. Penzias

The Warner & Swasey Company, Control Instrument Division

SUMMARY

The statistical band model was used to establish quantitative relationships for use in combustion gas analysis, in situ, for propulsion research applications. The necessary band model parameters, to relate infrared transmittance to CO_2 and H_2O concentrations were determined from 600°K to 2500°K at 4.40-μ for CO_2 and at 2.506-μ and 2.854-μ for H_2O. The band model parameters were obtained from transmittance measurements of furnace-heated gases and shock-heated gases.

A first step was taken in the use of high resolution water vapor measurements to obtain the desired band model parameters. Based on the high resolution measurements, a semi-theoretical single line approach was used to determine the temperature dependence of the water vapor strength parameters at 2.506-μ and 2.854-μ.

Improvements in the technique for determining H_2O concentrations, using integrated absorptance methods, and possible modifications of the statistical model relationship, were investigated. The statistical model proved to be adequate. Techniques for using integrated absorptance were established and integrated band model parameters were determined for H_2O at 2.5-μ and 2.8-μ at 637°K and 1273°K.

The effects of non-absorbing broadening gases on concentration determination were also considered.

the spectral interval. P_a is the pressure of absorber and P_b is the pressure of the non-absorbing broadening gas.

The statistical model parameters $S^\bullet/d$, $\gamma^\bullet_a/d$ and $\gamma^\bullet_b/d$ in Eqs. (2) and (3) are determined from transmittance measurements made at a specified wavelength and temperature. Equation (2) can be rewritten

$$\frac{\ln \frac{1}{\tau}}{P_a} = C\left(\frac{S^\bullet}{d}, \frac{\gamma^\bullet_a}{d}, \frac{\gamma^\bullet_b}{d}, m, \ell\right) \qquad (4)$$

where C, constant with pressure, is the slope of a straight line that results from plotting $\ln(1/\tau)$ vs P_a for a given mixture ratio and/or cell length. Since there are three unknowns, transmittance measurements at three mixture ratios and/or cell lengths must be made and the values of C determined in order to determine the unknown parameters.

From Eqs. (2) and (4) we see that the equations to be solved have the following form

$$C_i = 2\pi\left[\frac{\gamma^\bullet_a}{d} + m_i \frac{\gamma^\bullet_b}{d}\right] f\left(\frac{\left(\frac{S^\bullet}{d}\right) \ell_i}{2\pi\left[\left(\frac{\gamma^\bullet_a}{d}\right) + m_i \left(\frac{\gamma^\bullet_b}{d}\right)\right]}\right) \qquad (5)$$

where $i = 1, 2, 3$ correspond to 3 measurements made at three different mixture ratios and cell lengths. An iterative method for the solution of these equations has been described by Babrov (8).

To use the statistical model for determining concentration of gases in a mixture, the band model parameters must be known over the temperature range of interest. In principle, one could obtain the band model parameters from only three measurements. The accuracy of the values obtained, however, depends on the sensitivity of the particular experiments conducted. In practice the following experimental conditions are used to obtain maximum accuracy.

1) Pure absorber and long path length - high x ($x > 5$).

2) Large pressure of broadener relative to the pressure of absorber, short path length - low x ($x < 0.1$).

pertinent to the present work are given below. Previous research (4) established that the statistical model is applicable to water vapor and CO_2 transmittance data. The statistical model relates the transmittance τ to absorbing path length ℓ, absorber pressure P_a and foreign gas pressure P_b, using three spectroscopic parameters. The transmittance τ is defined by

$$\tau = \frac{I}{I_o} \tag{1}$$

where I_o is the relative intensity of an incident beam of infrared radiation of narrow spectral width centered at ν, a characteristic vibration frequency of the gas, and I is the relative intensity of the transmitted beam emerging from the gas.

The statistical model relationships, including the effect of foreign gas broadening are as follows:

$$\ln \frac{1}{\tau} = 2\pi P_a \left[\left(\frac{\gamma^\bullet_a}{d} \right) + m \left(\frac{\gamma^\bullet_b}{d} \right) \right] f(x) \tag{2}$$

where

$$m = \frac{P_b}{P_a}$$

$$f(x) = xe^{-x} \left[J_o(ix) - i\, J_1(ix) \right]$$

$J_o(ix)$ and $J_1(ix)$ are Bessel functions with imaginary arguments,

$$x = \frac{\left(\frac{S^\bullet}{d} \right) \ell}{2\pi \left[\left(\frac{\gamma^\bullet_a}{d} \right) + m \left(\frac{\gamma^\bullet_b}{d} \right) \right]} , \tag{3}$$

$S^\bullet/d$ is the line strength parameter, $\gamma^\bullet_a/d$ and $\gamma^\bullet_b/d$ are the half-width parameters for self-broadening and foreign gas broadening, respectively, per unit pressure and averaged over

extent to the foreign gas broadening.

The above discussion pertains to transmittance measurements made at the same wavelength and temperature. To obtain the temperature variation of transmittance as a function of path length, pressure and concentration, it is necessary to perform a series of measurements as described above at various temperatures and obtain the band model parameters. The parameters can then be graphed as a function of temperature, for interpolation.

The techniques described above have been used to obtain band model parameters for CO_2 and H_2O and are described in sections IV and V. The experimental approach to obtaining the necessary transmittance data are strongly influenced by the accuracy requirements given above.

III. INVESTIGATION OF IMPROVEMENT OF WATER VAPOR BAND MODEL RELATIONSHIPS

Improvement of the band model procedures for relating water vapor transmittance to optical density were investigated. Modification of the statistical band model representation of water vapor using a finite instead of an infinite number of lines in the spectral interval was considered because of the limited number of lines contributing to the H_2O peak transmittance in the wavelength intervals studied. The statistical model relationship for a finite number of lines is (2)

$$N\left[1 - (\tau)^{\frac{1}{N}}\right] = 2\pi P_a \left[\frac{\gamma^{\bullet}_a}{d} + m\frac{\gamma^{\bullet}_b}{d}\right] f(x) \qquad (9)$$

where N is the number of lines in the spectral interval. For a given cell length and mixture ratio, a plot of $N\left[1 - (\tau)^{\frac{1}{N}}\right]$ vs P_a should result in a straight line if this relationship is valid for the water vapor transmittance data. Several values of N were tried and it was found that the above relationship did not improve the fit of the experimental data over that previously obtained for the statistical model with an infinite number of lines. Therefore, the statistical model relationship described in Section II was used for water vapor transmittance measurements.

3) Moderate pressure of broadener relative to pressure of absorber, long path length - high x.

The accuracy of $S^\bullet/d$ depends on measurements 2 and 3. The greater the ratio of high x to low x, the greater the accuracy of the value determined for $S^\bullet/d$. The ratio of path length in the two experiments should be as great as possible. This difference in path length is desirable because one cannot achieve optimum accuracy by manipulation of mixture ratio alone.

The value of $\gamma^\bullet_a/d$ is determined from the self-broadening experiment 1 above; the experiment with pure absorber. In this experiment, x is high and Eq. (2) can be approximated by

$$\ln \frac{1}{\tau} = 2 P_a \left[\left(\frac{S^\bullet}{d}\right) \left(\frac{\gamma^\bullet_a}{d}\right) \ell \right] \quad . \tag{6}$$

Therefore, the relative error in the half width parameter is twice the relative error in $\ln \frac{1}{\tau}$.

The accuracy of $\gamma^\bullet_b/d$ is influenced by the mixture ratio used in experiment 3, the high x measurement. The relationship between the relative error $\ln \frac{1}{\tau}$ and the relative error in $\gamma^\bullet_b/d$ is given by

$$\frac{\Delta \left(\frac{\gamma^\bullet_b}{d}\right)}{\gamma^\bullet_b/d} = \phi_m \frac{\Delta \left(\ln \frac{1}{\tau}\right)}{\ln \frac{1}{\tau}} \tag{7}$$

where

$$\phi_m = \left[1 + \frac{\gamma^\bullet_a/d}{\gamma^\bullet_b/d} \left(\frac{1}{m}\right)\right] \left(\frac{f(x)}{f(x) - x f'(x)} \right) \quad . \tag{8}$$

It can be seen from Eq. (8) that as m goes to zero the error in $\gamma^\bullet_b/d$ increases rapidly. Therefore, to avoid large errors in the determination of $\gamma^\bullet_b/d$ the mixture ratio used should be chosen so that the total half-width is due to a significant

IV. DETERMINATION OF CO_2 STATISTICAL MODEL PARAMETERS

The statistical model parameters, to relate spectral transmittance to CO_2 concentration, were obtained at 4.40-μ. This wavelength was selected because: there is no interference from atmospheric CO_2, the transmittance is lowest (highest absorptance) at this wavelength, and there is least interference from CO (4.6-μ fundamental band) and H_2O (6-μ band) which may be present in combustion gases.

The CO_2 band model parameters were obtained from transmittance measurements of hot CO_2 using furnace heated gas cells and a shock tube. The experimental systems used to measure the infrared transmittance of CO_2 have been previously described (3,4,9). The system previously used to measure shock velocities was improved.

The band model parameters obtained from these measurements, over the temperature range from 600°K to 2500°K are shown in Figs. 1 and 2. The strength parameter is plotted against temperature in Fig. 1. Similar data for the half-width parameters are shown in Fig. 2, where the ratio of the half-width parameter at temperature T to its values at 1273°K is plotted against temperature. Note that the half-width parameter increases with temperature, although in general, one expects the half-width of a single line to decrease with the increasing temperature. This apparently anomalous behavior of the CO_2 half-width parameter is due to the increasing number of hot bands and the resulting decrease in the mean line spacing. The half-width of a line may be decreasing with increasing temperature, but the mean line spacing is decreasing more rapidly.

The data between 600°K and 1273°K were obtained from measurements using furnace-gas cell-spectrometer system (3). Above 1273°K, the shock tube system (described in ref. 4), was used to determine the strength parameter. These measurements were made under low x conditions (short path and large pressure of broadener relative to pressure of absorber). It is possible to determine S°/d from these data since at low x, f(x) approximately equals x. Thus Eq. (2) reduces to

$$\ln \frac{1}{\tau} = \frac{S^\circ}{d} P_a \ell \quad . \qquad (10)$$

To obtain the half-width parameters at higher temperatures, high x (long path) measurements are required. Since the use of a sufficiently large diameter low pressure section is impractical, a multiple pass optical system was designed to fit into the existing shock tube system to provide a path

length suitable for obtaining high x measurements. The multiple pass optical system is shown schematically in Fig. 3. The optical system consists of two spherical calcium fluoride mirrors which are substituted for the shock tube windows previously used in the low x measurements. Each mirror is aluminized over its entire surface except for a small portion in the center of the mirror. Energy from the source unit is focused at this transparent portion, and after three passes is refocussed at the transparent section of the second mirror. The corner reflector, placed behind this mirror, displaces the light and returns it for another three passes to the opening in the first mirror. Thus, six traverses of the optical path result. A three-pass system is also illustrated in Fig. 3. The transmission of the six-pass optical system was compared to the transmission obtained using the sapphire windows in the low x experiments. The globar source intensity was reduced by three-quarters (i.e. transmission = .25). This compares favorably with the theoretically predicted transmittance of 0.28.

To accurately measure the transmittance over the same spectral interval used to obtain the low x data (spectroradiometer mechanical slit widths of 0.5 mm and 1.0 mm), a source more intense than a globar is required. Two practical infrared sources which can be used are either a Nernst glower or a carbon arc. At 4.40-μ the intensity of a Nernst glower is about 3 times that of a globar. For a carbon arc (operating at 3000°K) this ratio is 7.

Thus, the use of the six-pass optical system with a high intensity infrared source is a practical arrangement for achieving a long path in a shock tube system of conventional dimensions. The optical path length in our shock tube system is 6.56 cm (2.6 inches). This provides a path length of 39.4 cm using the six-pass system.

V. DETERMINATION OF H_2O STATISTICAL MODEL PARAMETERS

To determine water vapor band model parameters, regions where the water vapor absorptance is strong (i.e. transmittance is low) must be sought. This is complicated by the presence of water vapor in the atmosphere which must be eliminated from the optical path. This interference can be minimized by either evacuating, or flushing the system with an inert gas such as nitrogen. For practical application in combustion studies, flushing the optical path with dry nitrogen is preferred.

When the optical path was flushed with dry nitrogen, interference from atmospheric H_2O was eliminated in two wavelength regions, at 2.506-μ and 2.854-μ, where the hot water vapor absorptances were relatively strong. The transmittance is lower at 2.854-μ, than at 2.506-μ, which reduces the

experimental error for transmittance measurements at low water vapor concentrations. However, at 2.854-μ, CO_2 also has an absorption band. Therefore, when CO_2 is present in the combustion gas stream, measurements must be made at 2.506-μ, where CO_2 does not interfere. Because of interest in hydrogen-air combustion, it was felt that the additional effort in obtaining data at two wavelengths is justified. Typical water vapor spectra at 2.506-μ and 2.854-μ are shown in Figs. 4 and 5 respectively. The band model parameters were obtained from this type of transmittance data.

Measurement of water vapor transmittances are strongly dependent upon the spectral resolving power of the instrument used to obtain the data. The narrower the spectral slit width, the higher the measured absorptance. The spectra illustrated in Figs. 4 and 5 were obtained with a spectral slit width of approximately 2 cm^{-1}, which is a practical upper limit to the resolution that can readily be achieved with standard grating instrumentation. Accordingly, this resolution was used to obtain the transmittance data for determining the band model parameters at 2.506-μ and 2.854-μ. The peak transmittances were measured at the points shown in Figs. 4 and 5. When these data are to be applied to determining water vapor concentrations in situ, the same spectral resolution must be used. Because of the sensitivity of the transmittance measurement to instrument properties, the use of integrated absorptance rather than peak transmittance measurements was investigated. This is described in Section VI.

Using the techniques described in Section II above, water vapor transmittances were measured at 2.506-μ and 2.854-μ at 1273°K and 637°K using furnace heated gas cells. The furnace-gas cell-spectrometer system previously used (4) limited the high x water vapor transmittance measurements to an eight-inch path length. This experimental apparatus was modified to permit measurements to be made for path lengths up to 48 inches, which improves the accuracy of the determination of the half-width parameters. The modified furnace-gas cell-system consists of two furnaces in series with a triple pass optical system for each furnace. (The triple-pass optical system is shown schematically in Fig. 3.) Thus, when an 8-inch cell is placed in each furnace a total path length of 48 inches is obtainable. The experimental setup is shown in Fig. 6.

Using the water vapor transmittance data obtained with this modified system, the statistical model parameters were determined at 2.506-μ and 2.854-μ. The results are presented in Table 1. Note the differences between the half-width parameters and those previously obtained (4) at 2.854-μ. These differences are due to the shorter path length used in the previous measurements. The 3% change in the strength parameter

is due to the difference in the spectral resolution used to obtain this new data. While this is a small difference, it indicates the need to match the spectral slit width when applying these data to determining water vapor concentrations.

To obtain water vapor band model parameters at temperatures higher than 1273°K (the limit of standard commercial furnaces) either shock tubes or burners must be used. Burners are limited because of the difficulty in obtaining isothermal samples and uncertainties in the isothermal path length. In addition it is difficult to vary the temperature, path length, and mixture ratio over the range required by the band model fitting technique described in Section II. Shock tubes have the advantage in ease of controlling concentrations and temperatures as well as having a clearly defined path length. However, because of the short test time available, measurement techniques are different than those employed in the usual steady state gas cell measurements. The need to use a non-synchronous detection system limits the accuracy of the transmittance measurements. The additional requirement to maintain the narrow spectral slit width, limits the energy collected by the spectrometer.

Because of the experimental obstacles in obtaining water vapor transmittance data above 1273°K, an alternative approach for determining the band model strength parameter, as a function of temperature, was used. Twelve lines contribute to the peak transmittance at 2.854-μ (3503 cm^{-1} group) and 8 lines contribute to the peak transmittance at 2.506-μ (3990 cm^{-1} group). If the strength of each of these individual lines were known at one temperature, it would be possible to calculate the line strengths at any other temperature. This information would allow us to determine the temperature dependence of the strength parameter, thereby greatly reducing the number of experimental calibration measurements required. Theoretical calculations of water vapor line strengths in the 2.7-μ band have been made (10,11), however, experimental measurements to verify these calculations were nonexistant. To experimentally determine the strengths of the water vapor lines in the two wavelength regions of interest to this study, high resolution measurements were made using the high resolution spectrometer available in this laboratory.

The high resolution spectrometer system consists of a vacuum monochromator, detector section and vacuum source unit. The monochromator is of Czerny-Turner design with a 1.5 meter focal length employing a rectangular grating having a ruled area of 154 mm x 206 mm with 150 lines/mm and blazed at 6.0-μ in the first order. The monochromator can be evacuated to a pressure of less than .5-μ Hg using an oil diffusion pump and a liquid nitrogen cooled trap. The vacuum source unit contains a furnace to heat the gas samples contained in a gas cell and a

Nernst glower as the infrared source for transmission measurement. The residual water vapor in the source unit is eliminated through the use of combined evacuation and flushing with nitrogen. The interfering atmospheric water vapor lines have been completely eliminated in the spectral intervals of interest (i.e. 2.506-μ and 2.856-μ). A gas handling system for introducing water vapor into the gas cells (10) is employed in connection with the source unit. The monochromator section of the high resolution spectrometer is shown in Fig. 7 and the vacuum source unit is shown in Fig. 8.

The resolution of the spectrometer system is better than 0.22 cm^{-1} at 3899 cm^{-1}. We succeeded in separating the water vapor spectrum at 2.506-μ and 2.856-μ into individual lines and into several lines grouped together. These are tabulated in Table II with the isolated lines and line groups indicated.

Water vapor absorptance measurements, for the lines grouped at 2.506-μ and 2.856-μ, were made at 423°K and 1123°K using a 1½-inch gas cell. From these measurements, integrated absorptances were determined for the individual lines and line groups listed in Table II. Using standard techniques the strength of the individual lines in the two wavelength groups were then calculated and compared to theoretical strengths predicted by Maclay (10). The results are shown in Table III.

For the lines grouped at 3503 cm^{-1} there was good agreement between the theoretical and experimentally determined line strengths at 423°K and poor agreement at 1123°K. For the 3990 cm^{-1} group of lines, there was good agreement at 1123°K and poor agreement at 423°K. It may be argued that the measured values represent the true line strengths as they have been determined experimentally. However, when the 423°K data was extrapolated to 1123°K and the 1123°K data extrapolated to 423°K, inconsistencies were revealed. A reappraisal of the experimental setup indicated possible errors in measuring the furnace temperature, which could account for the discrepancy between theory and experiment.

Based on the high resolution measurements, a semi-theoretical single line approach (4) was used to determine the temperature dependence of the water vapor strength parameters. The high resolution water vapor measurements were used to determine the relative contributions of the lines to the peak transmittance for the group of lines at 2.506-μ and 2.854-μ. The lower state energies of these lines were then mathematically averaged to yield the temperature dependence relationship for the strength parameter. The results are as follows:

At 2.506-μ

$$\frac{S^\bullet}{d}(T) = \frac{S^\bullet}{d}(1273°K)\left\{0.66\exp\left[-2557\left(\frac{1}{T}-\frac{1}{1273}\right)\right] + 0.34\exp\left[-1838\left(\frac{1}{T}-\frac{1}{1273}\right)\right]\right\}\left(\frac{1273}{T}\right)^{5/2}\frac{Q_v(1273)}{Q_v(T)} \qquad (11)$$

At 2.854-μ

$$\frac{S^\bullet}{d}(T) = \frac{S^\bullet}{d}(1273°K)\left\{\exp\left[-2160\left(\frac{1}{T}-\frac{1}{1273}\right)\right]\right\}\left(\frac{1273}{T}\right)^{5/2}\frac{Q_v(1273)}{Q_v(T)} \qquad (12)$$

where T = temperature °K and Q_v = vibrational partition function. Q_v plotted against temperature to 2000°K is given in Fig. 9. The data of Benedict (12) can be used to obtain Q_v at higher temperatures.

The accuracies of Eqs. (11) and (12) were checked by comparing $\frac{S^\bullet}{d}$ values calculated from these equations to measured values at 637°K and 2000°K. The comparison is shown in Table IV. The agreement varied from 3% to 12% over the temperature range of 637°K to 2000°K. It is estimated that Eqs. (11) and (12) are accurate to within ± 10% below 1273°K and within ± 20% above 1273°K.

VI. USE OF INTEGRATED ABSORPTANCE FOR WATER VAPOR CONCENTRATION DETERMINATION

As mentioned in Section V, water vapor transmittance measurements are influenced by instrumental affects. Accordingly, the use of integrated absorptance rather than peak transmittance, for predicting water vapor concentrations, was investigated. Using integrated absorptance eliminates the necessity of exactly matching the spectral slit width to that used to determine the statistical model parameters when applying the data to determining water vapor concentrations in situ. The spectral slit width

may be somewhat larger or smaller than 2 cm^{-1}. The spectral slit width can vary from 1 to 5 cm^{-1} without affecting the integrated absorptance. It has been shown that the integrated absorptance is insensitive to a change in spectral resolution as long as the absorptance is at or near zero at the end points of the integration (13).

The statistical band model relationships given in Section II, Eqs. (1) and (2) can be used to relate the integrated absorptance (integrated transmittance) to water vapor concentration, path length and total pressure. To obtain the desired integrated absorptance data, the spectral interval of interest is scanned and the area under the transmittance curve is measured. This is illustrated schematically in Fig. 10. Referring to Fig. 10, the shaded areas are measured with a planimeter and the integrated absorptance $\bar{A}$ is given by

$$\bar{A} = \frac{u}{u + T} \tag{13}$$

and

$$\bar{\tau} = 1 - \bar{A} \quad . \tag{14}$$

The $\bar{\tau}$ thus determined is used in the place of τ in Eq. (1). To determine the strength and half-width parameters, the techniques and experiments described in Section II are used with the integrated transmittance data. The difference is that the band model parameters obtained from peak transmittance measurements will differ from those obtained using the integrated transmittance data.

Using water vapor transmittance data obtained with the furnace-gas cell-spectrometer system, integrated transmittance band model parameters were determined. The limits of wavelength integration are indicated by the dashed lines in Figs. 4 and 5 for the 2.5-μ (3990 cm^{-1}) and 2.86-μ (3503 cm^{-1}) wavelength regions. The wavelength interval is approximately 9 cm^{-1}. The resultant band model parameters are tabulated below.

λ	int. $\frac{S^\bullet}{d}$	int. $\frac{\gamma^\bullet_a}{d}$	Temperature °K
2.5-μ interval	0.070	0.175	1273
2.5-μ interval	0.074	0.184	637
2.85-μ interval	0.125	0.287	1273
2.85-μ interval	0.137	0.338	637

The strength parameter temperature relationships given in Eqs. (11) and (12) of Section V cannot be used with the above integrated band model parameters because of the differences in the spectral interval.

At higher temperatures, integrated band model parameters could be obtained from shock tube measurements. For the CO_2 shock tube measurement, the minimum slit width that could be used with the spectroradiometer (9) using a globar source was 0.5 mm. To achieve a 9 wavenumber spectral slit width with this instrument the mechanical slit width must be 0.2 mm. This reduces the signal intensity by a factor of 6.25. If a carbon arc is substituted for the globar, the source intensity is increased by a factor of twenty in the 2.7-μ region. Thus, the net improvement with a carbon arc source would be 3.2. The six-pass optical system must be used for the high x measurement. The transmission characteristics of this system are such that the source intensity is diminished by a factor of 3. The carbon arc still would provide sufficient intensity to permit the use of the six-pass system in the shock tube.

Because of the low absorptance characteristics of water vapor it would be desirable to increase the optical path of the shock tube. The shock tube low pressure section (driven section) could readily be increased to a diameter of 4 inches. This would result in a 24" path length for the high x measurements using the six-pass optical system.

If shock tube measurements of water vapor transmittance are made, the slit function of the monochromator must be rectangular. One is also faced with the experimental problem of introducing a known concentration of water vapor into the shock tube. While these are attendant problems, the use of a shock tube to obtain water vapor band model parameters at high temperature appears feasible.

where, P_S is the partial pressure of gas S required to give the same absorptance as that produced by a partial pressure, P_{N_2} of nitrogen when the absorber concentration is the same in the two samples. The summation in Eq. (16) is made for i^{th} species present in the sample other than nitrogen.

Relative (to nitrogen) foreign broadening coefficient data are presented in Table V. We have also listed the ratio of self-broadened half-width to nitrogen broadened half-width, sometimes called the self-broadening coefficient B (14), as a check of the consistency between our measurements and those of other investigators. The agreement is generally good.

VIII. CONCLUSIONS

The statistical band model relationship has been used to describe the CO_2 transmittance at 4.40-μ and the band model parameters have been determined over the temperature range from 600°K to 2500°K. The strength parameters have been determined to an accuracy of 5% over this temperature range. Half-width data have been obtained up to 1273°K. The possibilities of determining half-width data for CO_2 from shock tube measurements was explored and the experimental means for obtaining this data established. The use of a multiple pass optical system was shown to be practical for obtaining high x data with a shock tube system.

Water vapor absorptances have been measured in gas cells and the transmittance data fitted to the statistical band model at 2.506-μ and 2.856-μ at 637°K and 1273°K. Formulas were developed for extrapolating the strength parameter to higher temperatures. The accuracy of the temperature extrapolation was evaluated. A first step was taken in the use of high resolution water vapor measurements to obtain the desired band model parameters. The success of this approach would greatly reduce the number of experimental calibration measurements required to obtain these parameters.

Possible improvements in the statistical band model relationship for water vapor were investigated. The statistical model proved to be adequate.

To eliminate the influence of instrumental effects inherent in the use of peak transmittance measurements for determining water vapor concentrations, the use of integrated absorptance was investigated. The techniques for using integrated absorptance were established and integrated band model parameters were determined at 637°K and 1273°K. The use of shock tube measurements for obtaining integrated band model parameters at higher temperatures was evaluated and found to be feasible.

VII. BROADENING EFFECTS ON CONCENTRATION DETERMINATION

The effect of pressure broadening on the absorption lines due to the presence of species other than the absorber are included in the statistical model relationship by the foreign gas broadening half-width. In the CO_2 and water vapor measurements discussed above, the influence of nitrogen as the broadening agent was determined. It is possible to account for the presence of other broadening gases, using relative (to nitrogen) broadening in the statistical model relationships. The broadening effects of oxygen, water vapor, and helium on CO_2 absorptance, relative to nitrogen, have been previously determined (3). Similar measurements have been made by Birch et al (14) and Rusk (15).

In the statistical model relationships described in Section II, the half-width parameter γ/d for a binary mixture of absorber and broadener is given by

$$\frac{\gamma}{d} = P_a \left(\frac{\gamma^\bullet a}{d}\right) + P_b \left(\frac{\gamma^\bullet b}{d}\right) \quad . \tag{15}$$

Nitrogen was used as the broadener for the CO_2 and H_2O measurements described in Sections IV and V and $\frac{\gamma^\bullet b}{d}$ for nitrogen was determined. If there are several broadening gases present in the sample Eq. (15) can be written as

$$\frac{\gamma}{d} = P_a \left(\frac{\gamma^\bullet a}{d}\right) + \frac{\gamma^\bullet b}{d} \left[P_{N_2} + \sum_i F_i P_i\right] \tag{16}$$

where P_a is the pressure of absorber, $\frac{\gamma^\bullet a}{d}$ is the self-broadening half-width parameter, $\frac{\gamma^\bullet b}{d}$ is the nitrogen half-width parameter, P_{N_2} is the nitrogen pressure.

F is the relative (to nitrogen) foreign broadening coefficient of a non-absorbing gas S and is defined by

$$F = \frac{P_{N_2}}{P_S} \tag{17}$$

REFERENCES

1. G. J. Penzias and R. H. Tourin, Combustion & Flame 6, 147 (1962).

2. R. M. Goody, Atmospheric Radiation (Oxford University Press, London, 1964), pp. 122 to 170.

3. G. J. Penzias, G. J. Maclay, and H. J. Babrov, NASA CR-1, Final Report on Phase II of Contract NAS 3-1542 (1962).

4. G. J. Penzias and G. J. Maclay, NASA CR-54002, Final Report on Phase III, Contract NAS 3-1542, NASA Lewis Research Center, Cleveland, Ohio (1963).

5. G. J. Penzias and G. J. Maclay, Tenth Symposium (International) on Combustion (The Combustion Institute, Pittsburgh, 1965), p. 189.

6. G. N. Plass, J. Opt. Soc. Am. 48, 690 (1958).

7. U. P. Oppenheim, Ninth Symposium (International) on Combustion (1962), p. 96.

8. H. J. Babrov, Ph.D. Thesis, University of Pittsburgh, 1959; also available as AFOSR TR-59-207 (1959).

9. G. J. Penzias, S. A. Dolin, and H. A. Kruegle, Appl. Optics 5, 225 (1966).

10. G. J. Maclay, J. Chem. Phys. 43, 185 (1965).

11. D. M. Gates, R. F. Calfee, D. W. Hansen, and W. S. Benedict, Natl. Bur. Std. Monograph No. 71, August 1964.

12. W. S. Benedict et al, Natl. Bur. Std. Report No. 1123 (1951).

13. H. J. Babrov, J. Opt. Soc. Am. 53, 831 (1962).

14. D. E. Burch, E. B. Singleton, and D. Williams, Appl. Optics 1, 359 (1962).

15. J. R. Rusk, J. Chem. Phys. 42, 493 (1965).

16. D. K. Edwards, J. Opt. Soc. Am. 50, 617 (1960).

17. H. J. Babrov, G. Ameer, and W. Benesch, J. Chem. Phys. 33, 145 (1960).

The information obtained to date for CO_2 and water vapor provides a good beginning for applying this information to the determination of CO_2 and H_2O in combustion gases. The CO_2 data has previously been tested for determination of shock tube concentration. The H_2O data should prove useful for supersonic combustion studies. For this application, low x conditions should prevail and only the H_2O strength parameter is required.

The data contained in this report can be used to determine the applicability of infrared transmittance measurements for determining CO_2 or H_2O concentrations in situ for a particular application. For example, if nozzle recombination studies are being made, it is possible to estimate the transmittance for frozen and equilibrium conditions and evaluate the sensitivity of the infrared methods to distinguish between the two conditions.

TABLE I

Statistical Band Model Parameters for H_2O

$\lambda(\mu)$	ν cm^{-1}	S°/d	γ°_a/d	γ°_b/d	$T^\circ K$
2.506	3990	0.175	0.486	0.085	1273
2.506	3990	0.184	0.706		637
2.854	3504	0.311[a]	0.617[b]	0.12[c]	1273
2.854	3504	0.362	1.088		637

a) previous value 0.321 (4)

b) previous value 0.444 (4)

c) previous value 0.090 (4)

TABLE II

H_2O Lines Measured With High Resolution Spectrometer

a) Lines in the 3504 cm^{-1} group (2.854-μ).

ν cm^{-1}	
3499.73	single isolated line
3500.33	single isolated line
3501.02	single isolated line
3501.54, 3501.76	to be treated as single isolated line
3502.38, 3502.40	to be treated as single isolated line
3502.77, 3503.05, 3503.28	to be treated as single isolated line
3504.12	two lines at same ν can be considered as single isolated line
3504.74	single isolated line

b) Lines in the 3990 cm^{-1} group (2.506-μ).

3989.48, 3989.60, 3989.61, 3989.85	to be treated as single isolated line
3990.23, 3990.26, 3990.44	to be treated as single isolated line
3990.70	single isolated line

TABLE III

High Resolution Measurements

	Temp. 1123°K			Temp. 423°K		
ν	S°(theor)	S°(meas)	$\frac{S^\circ(\text{theor})}{S^\circ(\text{meas})}$	S°(theor)	S°(meas)	$\frac{S^\circ(\text{theor})}{S^\circ(\text{meas})}$
3504.12	.3909	.2486	1.57	.1940	.1704	1.14
3503.28	.0209	.0214	.98	.1542	.1115	1.38
3503.05	.0116	.0101	1.15			
3503.77	.2407	.2109	1.14	.1514	.1513	1.00
3502.40	.0867	.0561	1.54	.0461	.0478	0.96
3502.38	.2598	.1632	1.59	.1383	.1412	0.98
3501.76	.0821	.0613	1.34	.0525	.0524	1.0
3501.54	.2151	.1584	1.36	.1623	.1577	1.03
3500.33	.0367	.0502	0.73			
3499.73	.1674	.1238	1.35	.0987	.0891	1.11
3991.12				.0019	.0015	1.26
3990.70	.1362	.1173	1.16	.1211	.1237	0.98
3990.44	.0087	.0101	.86	.0082	.0109	.81
3990.26	.0985	.1170	.84	.0289	.0395	.73
3990.23	.0065	.0072	.90	.0104	.0154	.67
3989.85	.0233	.0235	1.0	.0082	.0121	.68
3989.61	.0255	.0256	1.0	.0080	.0121	.66
3989.60	.0274	.0276	1.0	.0102	.0149	.68
3989.48	.0763	.0777	0.98	.0239	.0375	.64

TABLE IV

Comparison of Calculated and Measured H_2O Strength Parameters

A. Comparison with gas cell measurements - accuracy $\pm$ 5%.

Wavelength	Temperature	S°/d (meas.)	S°/d [1]	Deviation
2.506-μ	637°K	0.362	0.388	7%
2.856-μ	637°K	0.184	0.201	9%

B. Comparison with unpublished data [2] - $\Delta\nu$ = 25 cm^{-1} accuracy $\pm$ 20%.

Wavelength	$\frac{S^\circ/d\ (2000^\circ K)}{S^\circ/d\ (1273^\circ K)}$ [1]	$\frac{S^\circ/d\ (2000^\circ K)}{S^\circ/d\ (1273^\circ K)}$ [2]	Deviation
2.506-μ	0.47	0.48	3%
2.856-μ	0.44	0.50	12%

1) Calculated from Equations (11) or (12).

2) Data supplied by NASA Marshall Space Flight Center.

TABLE V

Relative (to Nitrogen) Foreign Broadening Coefficients (F) and Self-Broadening to Nitrogen Broadening Coefficients (B)

Absorber	Broadener	B	F
CO_2 4.40-μ at 1273°K (3)		2.65	
"	O_2		0.91
"	H_2O		2 ± 0.4
"	H_e		1.0
All CO_2 bands at room temp. (14)		1.30 ± 0.08	
at room temp. (16)		2.0 ± 0.5p (where p is CO_2 pressure in atms.)	
CO_2 4.3-μ band (14) at room temp.	O_2		0.81
	H_e		0.59
	A		0.78
H_2O 2.506-μ at 1273°K		5.7	
H_2O 2.854-μ at 1273°K		5.1	
H_2O (15)		5.07	
H_2O (14)		5 ± 1.5	
H_2O (15)	O_2		0.72
H_2O (15)	CO_2		1.6
H_2O (15)	A		0.52
HCl (17)	CO_2		1.3 to 1.8

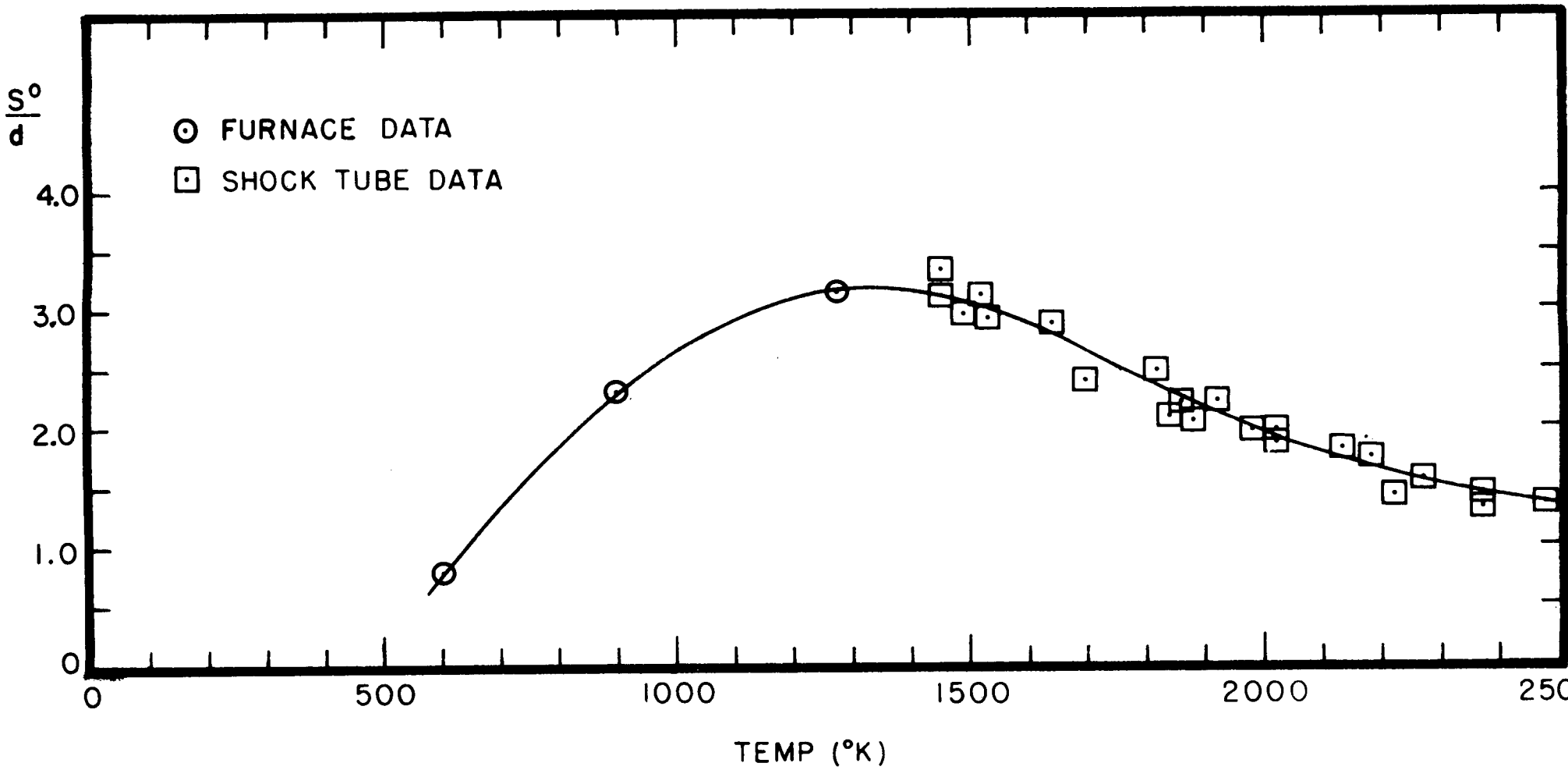

Fig. 1 CO_2 strength parameter S°/d, at 4.40-μ, plotted against temperature.

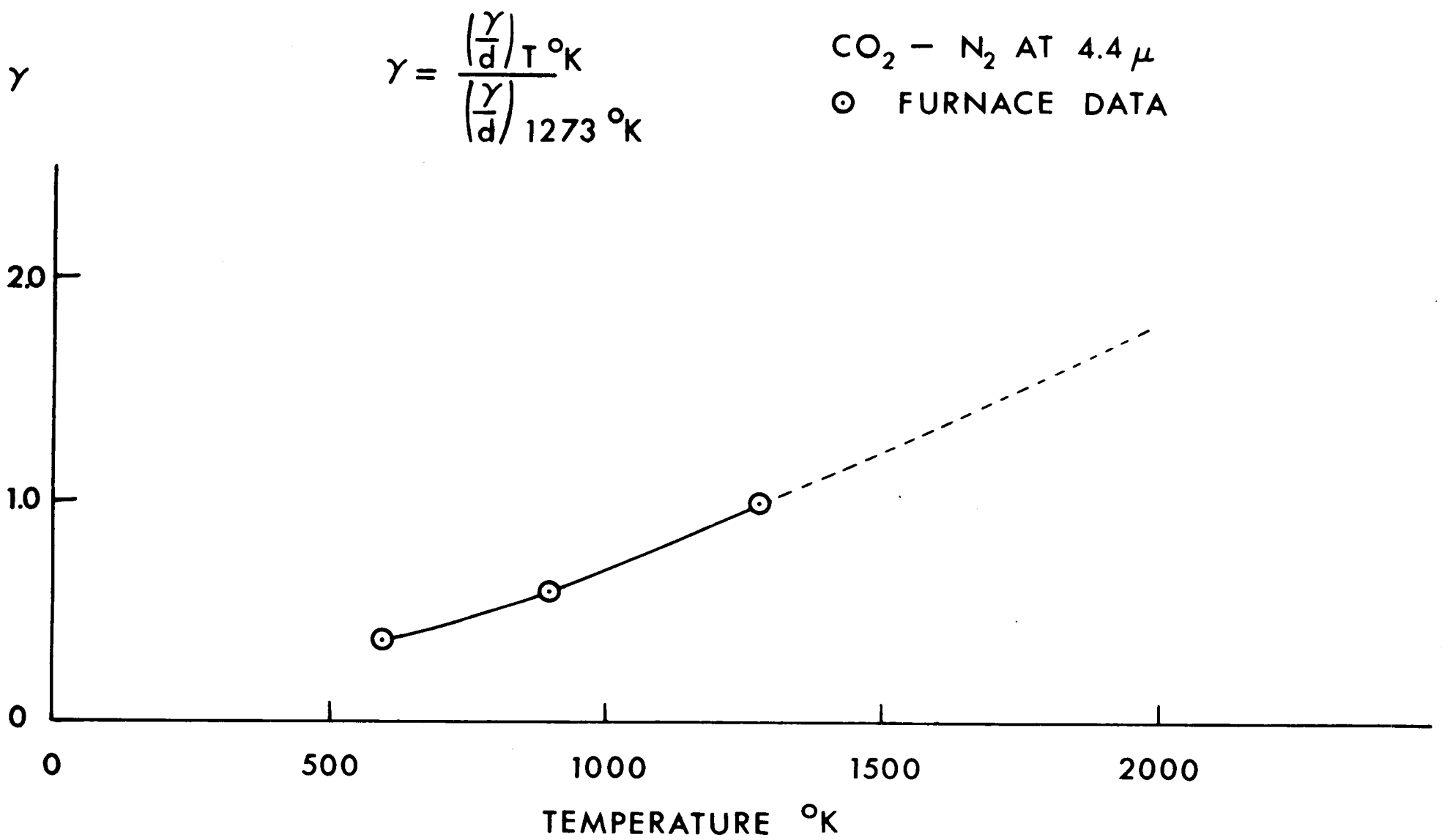

Fig. 2 Ratio of total half-width band model parameter $(\frac{\gamma^\bullet}{d})_T$, to half-width $(\frac{\gamma^\bullet}{d})_{1273}$ at 1273°K versus temperature.

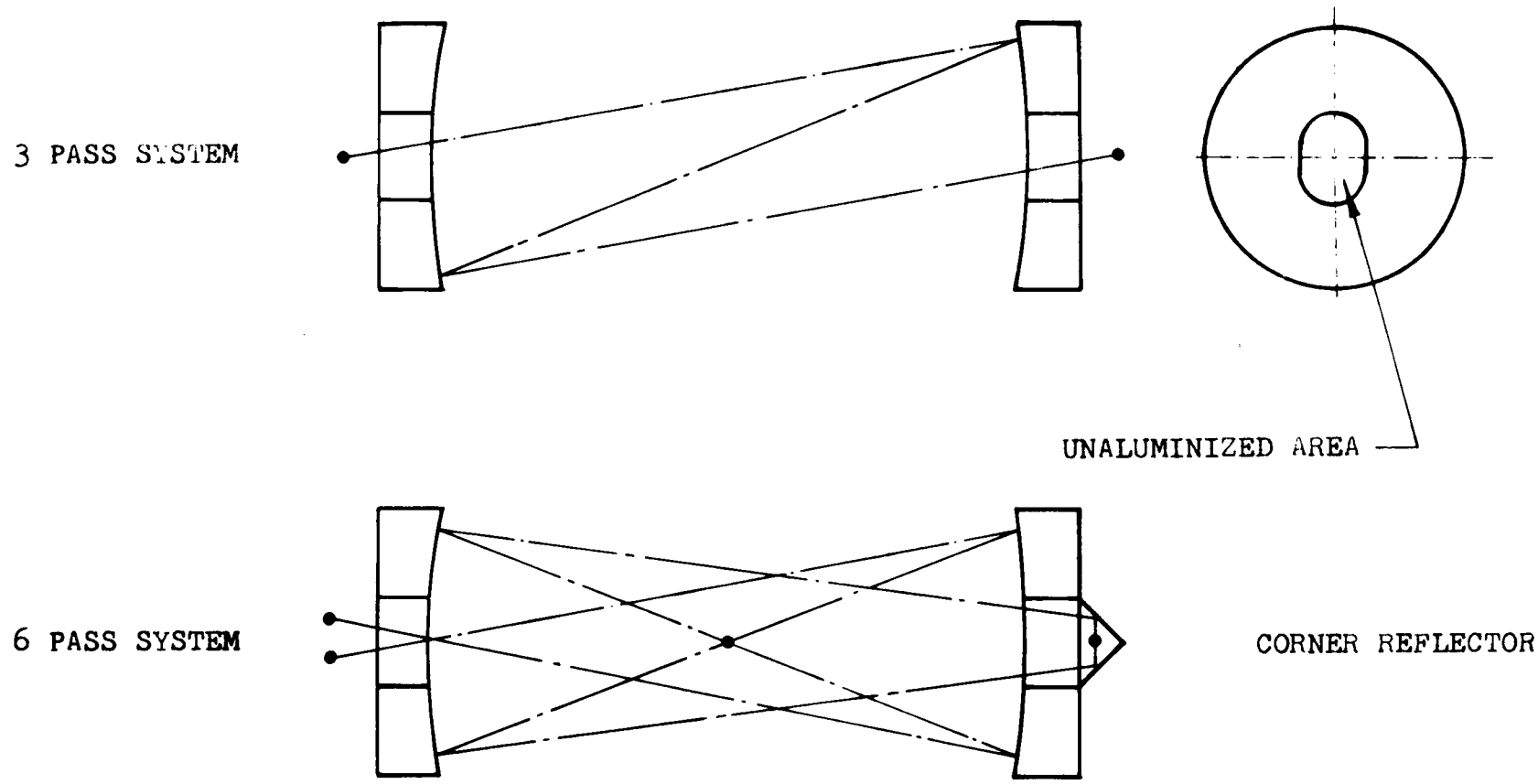

Fig. 3 Schematic diagram of multiple pass optical system for shock tube.

Fig. 4 Experimentally measured spectrum of water vapor near 2.506-μ (3990 cm^{-1}), at 1273°K and 312 Torr. The cell length is 8 in. The integrated absorptance was measured between the limits indicated by the dashed lines. Peak transmittance measurement indicated by arrow.

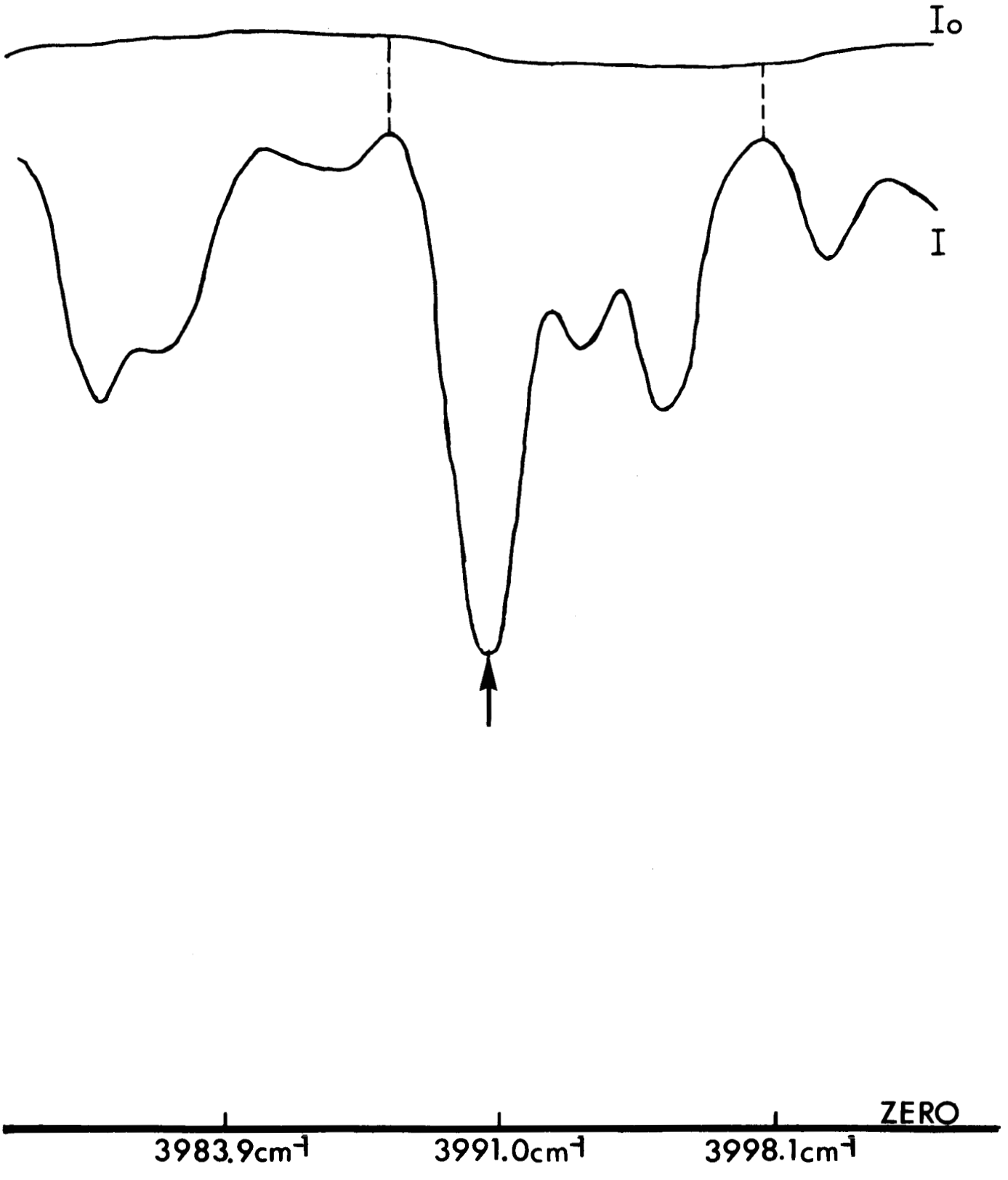

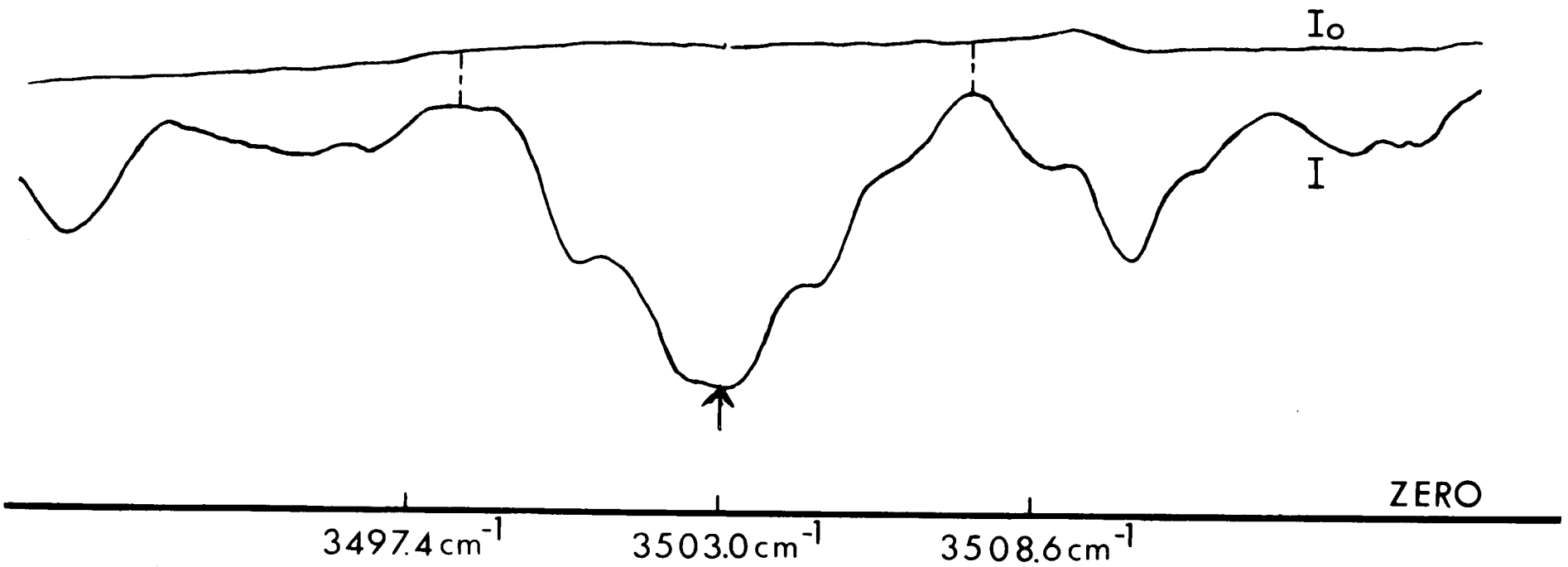

Fig. 5 Experimentally measured spectrum of water vapor near 2.854-μ (3503 cm^{-1}), at 1273°K and 312 Torr. The cell length is 8 in. The integrated absorptance was measured between the limits indicated by the dashed lines. Peak transmittance measurement indicated by arrow.

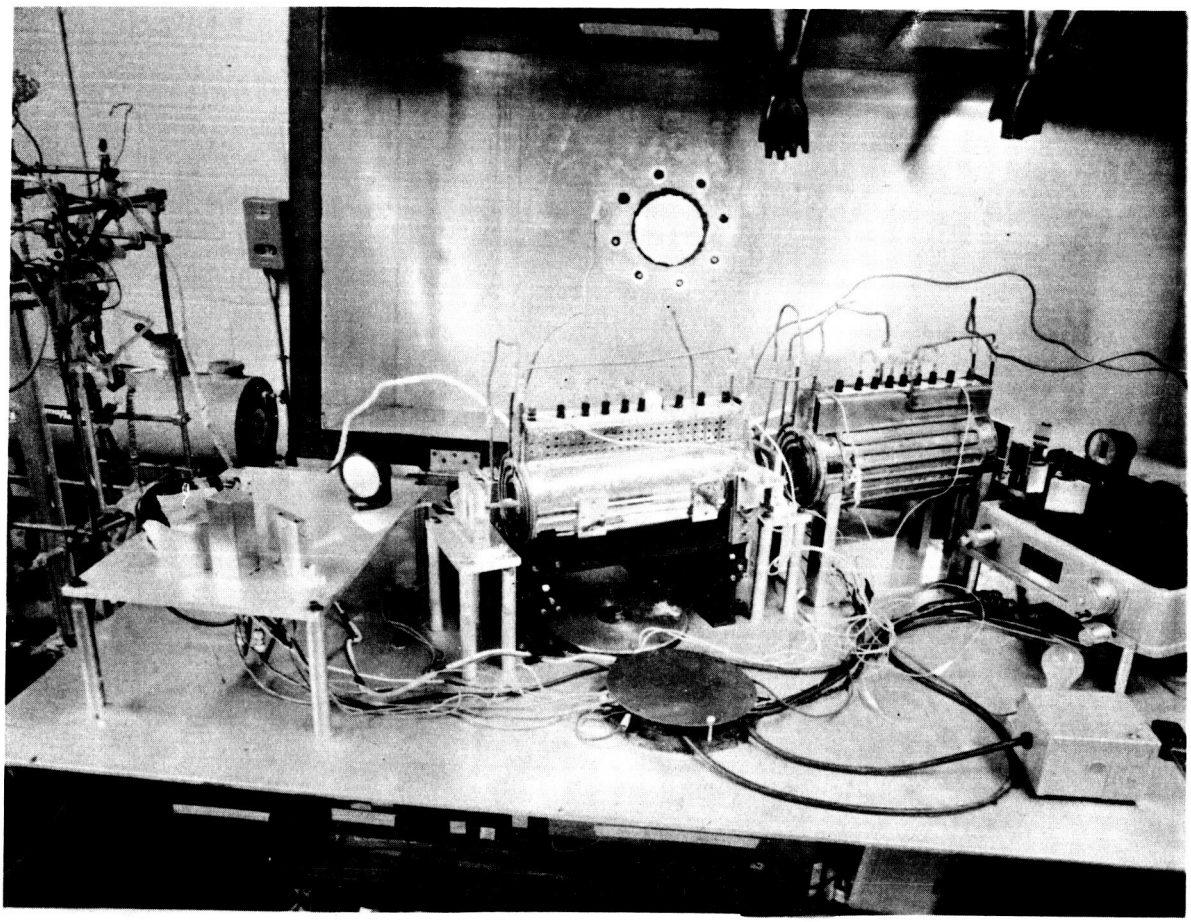

Fig. 6 Gas cell furnace spectrometer system. Two furnaces in series. Each furnace optical path triple passed.

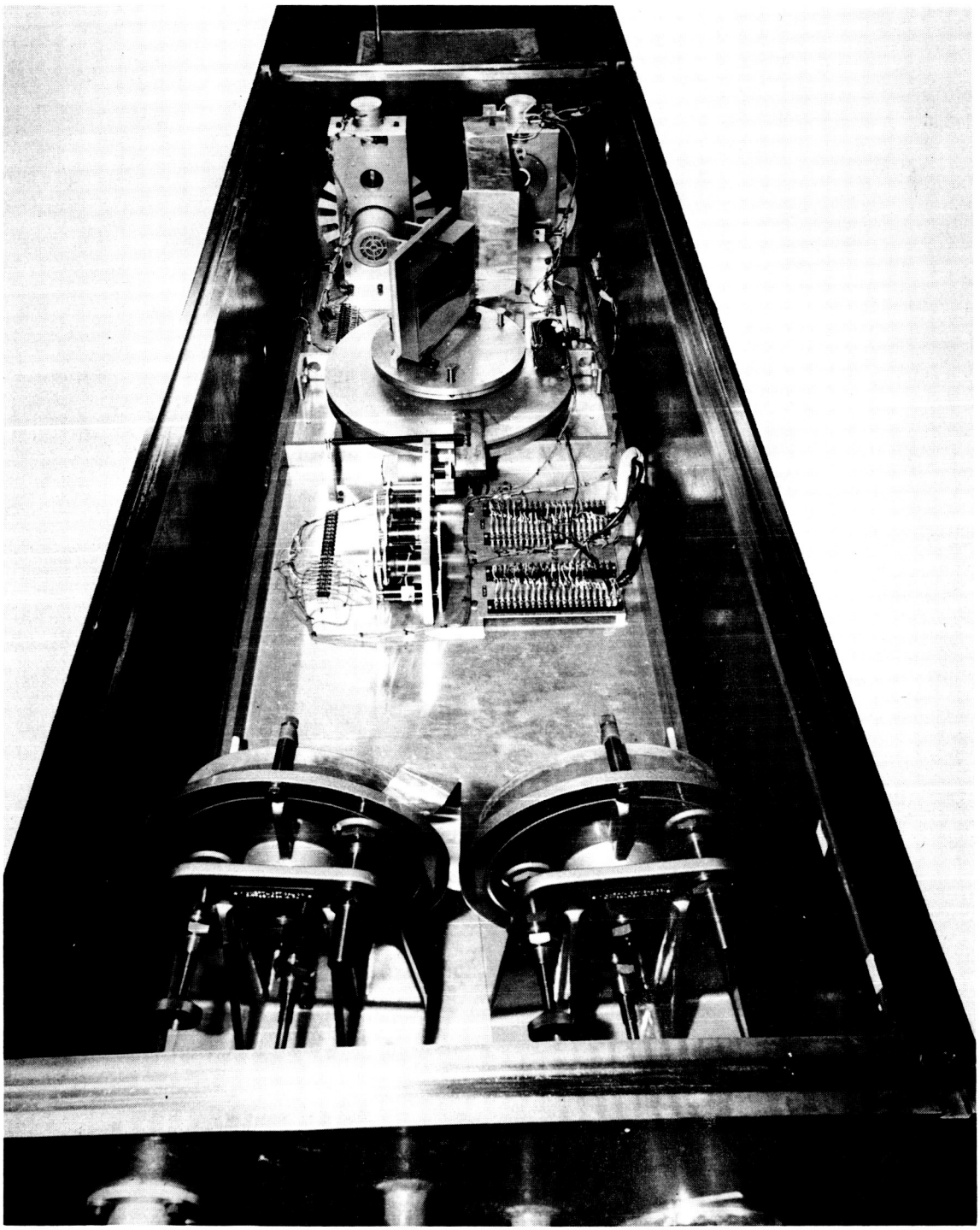

Fig. 7 High resolution vacuum monochromator.

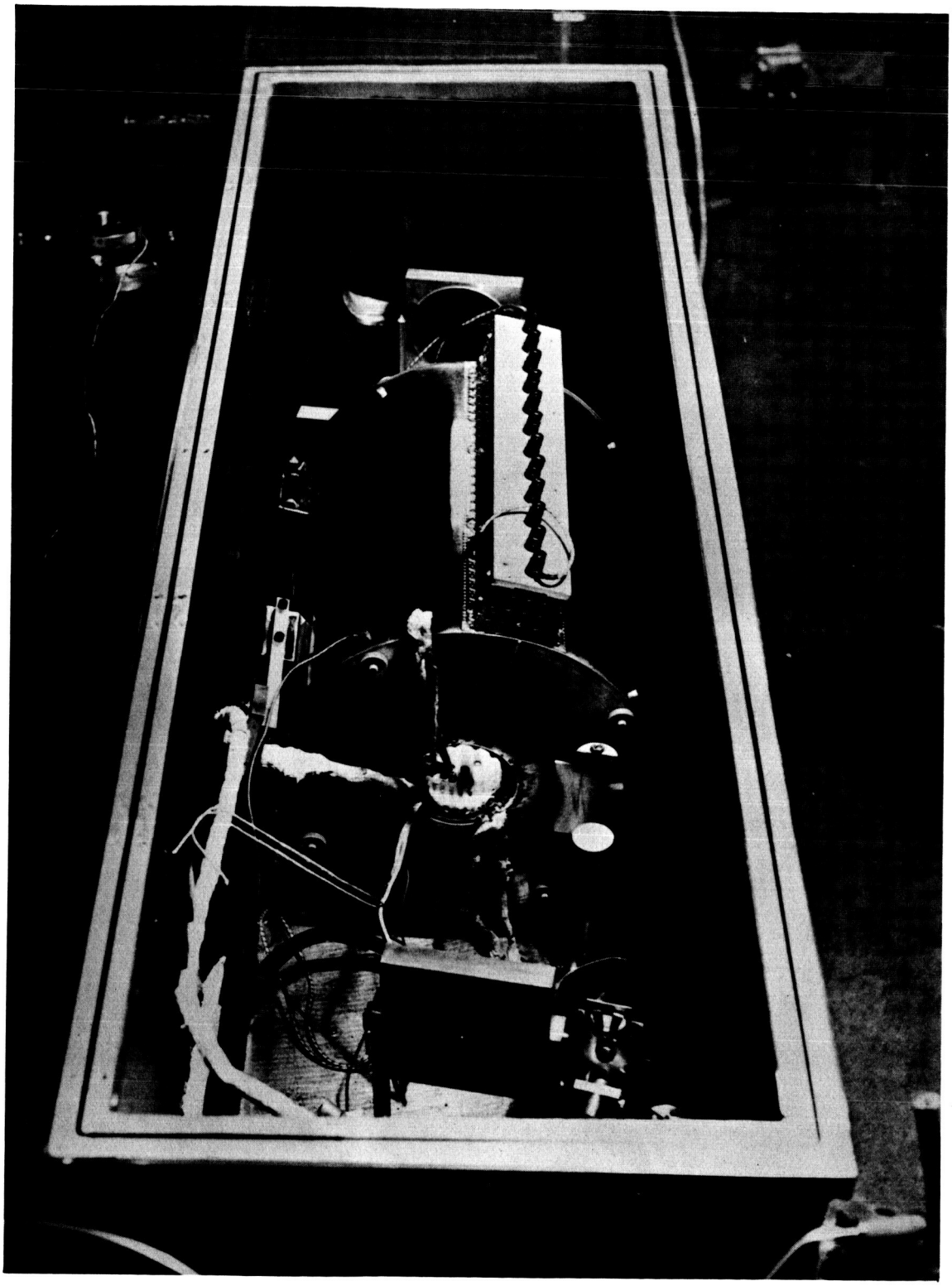

Fig. 8 Vacuum source unit of high resolution spectrometer system.

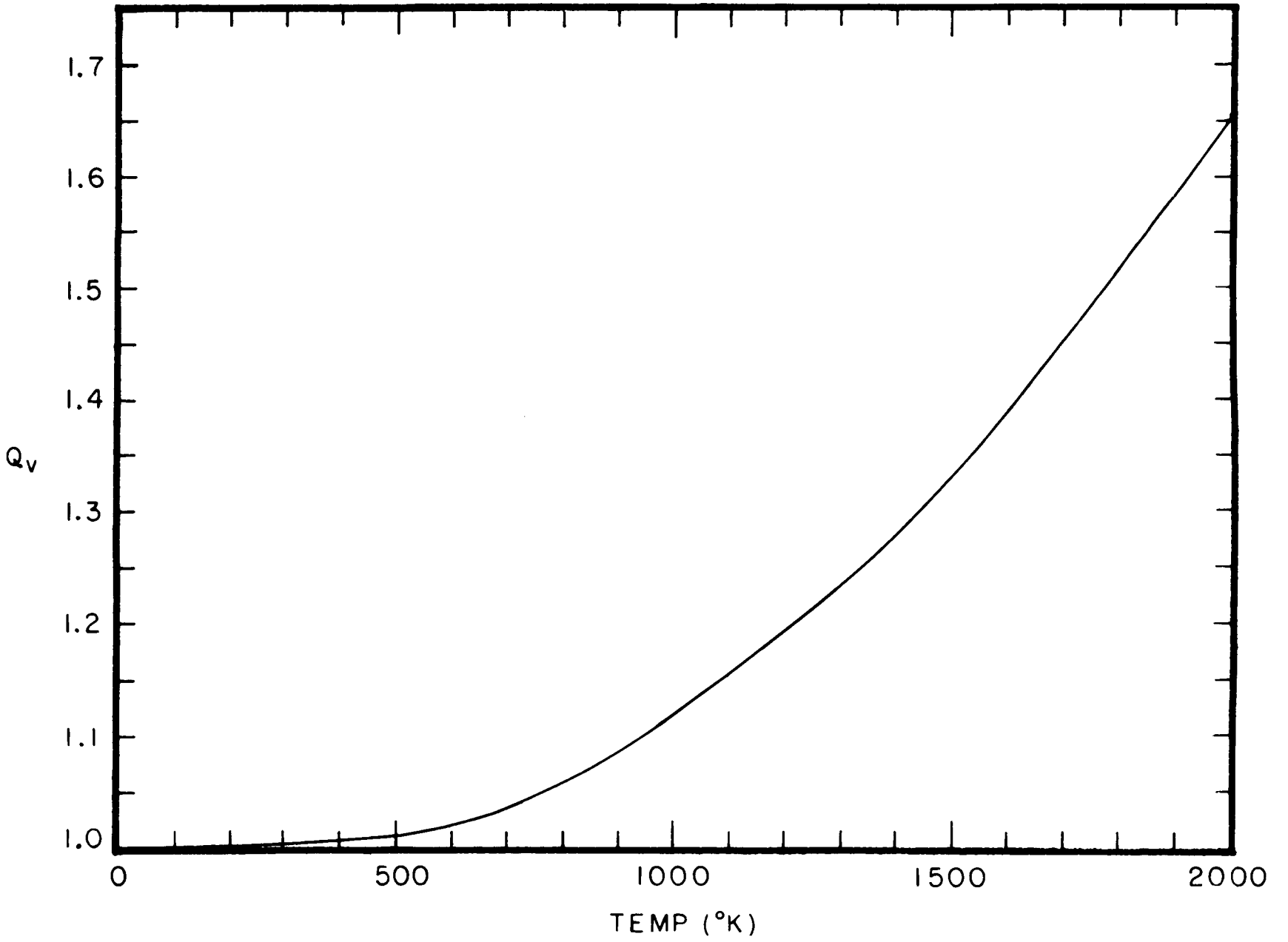

Fig. 9 H_2O vibrational partition function, Q_v, plotted against temperature.

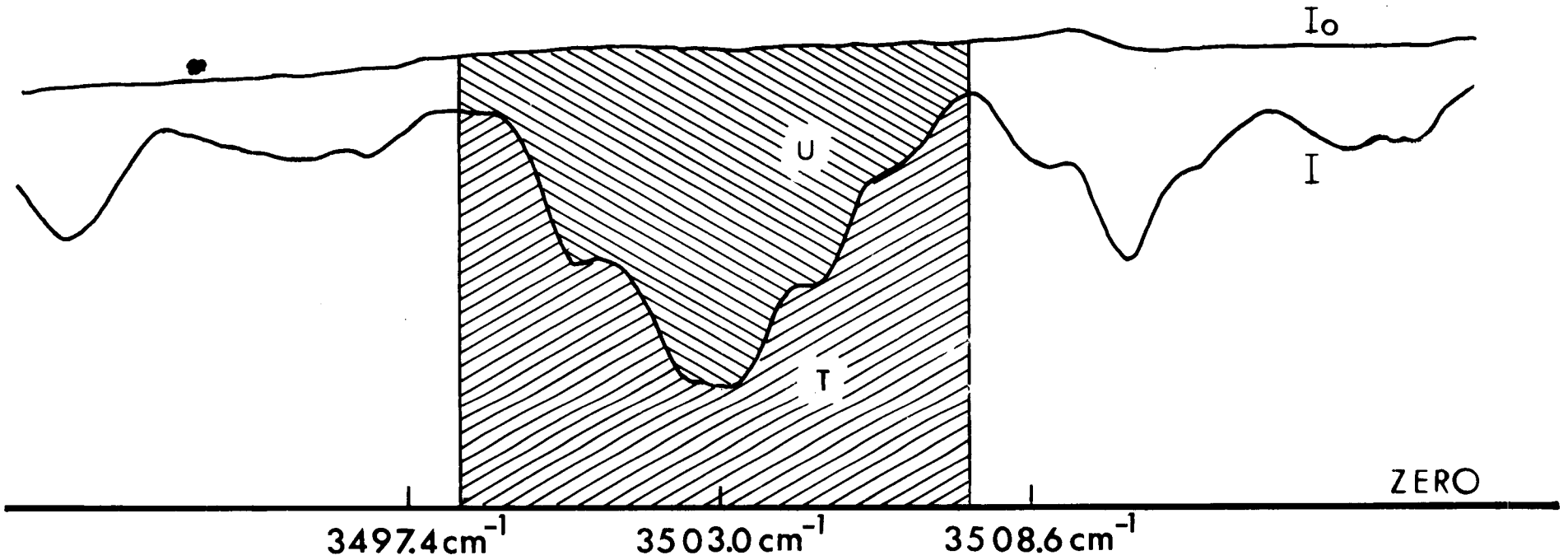

Fig. 10 Integrated transmittance data obtained by measuring shaded areas.